# Data Set User Manual (Web Version)

## GOCE+ GeoExplore

Document: DSUM (Web Version)

Issue: 1.1

Date: 10 July 2015

Deutsches Geodätisches Forschungsinstitut (DGFI), Munich, Germany

Christian-Albrechts-Universität zu Kiel

University of West Bohemia, Plzen, Czech Republic



# Document Information Sheet

| **Document Name** | | |
|---|---|---|
| Data Set User Manual (Web Version) | | |
| **Document ID** | **Issue** | **Date** |
| DSUM (Web Version) | 1.1 | 10/07/2015 |
| **Author** | **Institute** | |
| J. Bouman<br>M. Fuchs<br>J. Sebera | DGFI<br>DGFI<br>UWB | |

# Document Change Record

| **Issue** | **Date** | **Reason for change** | **Changed pages / paragraphs** |
|---|---|---|---|
| 1.0 | 21/11/2014 | New Issue for publication of gradient grids | All |
| 1.1 | 10/07/2015 | Header description updated<br>Topographic grids description added | Section 5.2<br>Section 5.2.4 |

# Contents

# 1 Introduction

The purpose of this document is to describe the gravity gradient products that are derived in the GOCE+ GeoExplore / GDC study. It is based on the more complete DSUM [RD-7] that describes other data sets as well.

# 2 Reference documents

[RD-1] PR-GOCE-DGFI-10/02: Tender, Heterogeneous gravity data combination for Earth interior and geophysical exploration research (Theme 2), Issue 1.0, 14 July 2010

[RD-2] DD-GOCE+-DNT-01: Requirement Baseline, Issue 2.1, 20 April 2012

[RD-3] DD-GOCE+-DNT-02: Preliminary Analysis Report, Issue 1.1, 24 April 2012

[RD-4] DD-GOCE+-DNT-03: Development and Validation Plan, Issue 1.0, 20 April 2012

[RD-5] DD-GOCE+-DNT-04: Algorithm Theoretical Basis Document, Issue 2.1, 21 November 2014

[RD-6] RP-GOCE+-DNT-05: Product Validation Report, Issue 2.1, 21 November 2014

[RD-7] MA-GOCE+-DNT-06: Data Set User Manual, Issue 1.2, 21 November 2014

[RD-8] PP-GOCE+-DNT-07: Promotion Plan, Issue 1.4, 31 May 2013

[RD-9] RP-GOCE+-DNT-08: Impact Assessment Report, Issue 1.1, 21 October 2014

[RD-10] RP-GOCE+-DNT-09: Scientific Roadmap, Issue 1.2, 21 November 2014

[RD-11] TN-GOCE+-DNT-10, LNOF to MRF gradient rotation, Issue 1.1, 08 February 2013

# 3 Background

GOCE data may improve the understanding and modelling of the Earth's interior and its dynamic processes, contributing to gain new insights into the geodynamics associated with the lithosphere, mantle composition and rheology, uplift and subduction processes. However, to achieve this challenging target, GOCE should be used in combination with additional data sources: e.g. magnetic, gravity and seismology in situ, airborne and satellite data sets.

The *overall objective of the study* is to combine GOCE gravity gradients with heterogeneous other satellite gravity information to arrive at a combined set of gravity gradients complementing (near)-surface data sets spanning all together scales from global down to 5 km useful for various geophysical applications and demonstrate their utility to complement additional data sources (e.g., magnetic, seismic) to enhance geophysical modelling and exploration.

# 4 Data models used

Below the use of global gravity models is described, specifically the global gravity field models in terms of spherical harmonics. They have three purposes:

1. They serve as background model to be subtracted from the gravity data (gradients, terrestrial data, etc.); as baseline we use maximum spherical harmonic degree and order 12 for that purpose (see the ATBD);
2. They serve as background model in the regional gravity field modelling; typically a model to spherical harmonic degree and order 60 is used;

3. They are used to compute model gravity gradients that aid in the enhancement of the GOCE gradients; GOCE-based or GRACE/GOCE-based models are being used.

Depending on the application it may be desirable to use a global gravity field model that includes only GOCE and/or GRACE data. Global gravity field models that include terrestrial gravity data have to be used with care because the GOCE-based gradients are to be combined with terrestrial data that we have available, and because terrestrial data may contain systematic errors.

The global gravity models that may be used in the project are:

| Model | Year | L-max | Input data | Reference |
|---|---|---|---|---|
| DIR R5 | 2014 | 300 | S(GOCE,Grace,Lageos) | Bruinsma et al, 2013 |
| TIM R5 | 2014 | 280 | S(GOCE) | Pail et al, 2011 |
| DIR R3 | 2011 | 240 | S(GOCE), GRACE as a priori | Bruinsma et al, 2010 |
| TIM R3 | 2011 | 250 | S(GOCE) | Pail et al, 2011 |
| GOCO02S | 2011 | 250 | S(GOCE,Grace,...) | Goiginger et al, 2011 |
| GOCO03s | 2012 | 250 | S(GOCE,Grace,...) | Mayer-Gürr et al, 2012 |
| EIGEN-6S | 2011 | 240 | S(GOCE,Grace,Lageos) | Förste et al, 2011 |
| EIGEN-6C | 2011 | 1420 | S(GOCE,Grace,Lageos),G,A | Förste et al, 2011 |
| EGM2008 | 2008 | 2190 | S(Grace),G,A | Pavlis et al, 2008 |

G = terrestrial gravity data included, A = altimeter data included.

All global gravity field models are downloaded from the ICGEM website and these are all in the ICGEM-format. See http://icgem.gfz-potsdam.de/ICGEM/ICGEM.html .

# 5 Data set documentation

## 5.1 Gravity gradients from GOCE and GRACE

The GOCE (Gravity field and steady state Ocean circulation explorer) started its mission on the 17th March 2009. First valid data products are available from the 1st of November 2009 onward and the last data products are available until November 2013 where GOCE disintegrated on the 11th November 2013. Chapter 5.1.1 describes the provided data format while Chapter 5.1.2 gives an overview of the monthly derived datasets and the GOCE measurement periods. The gradient accuracy including the data weaknesses and strengths are stated in section 5.1.6 and 5.1.3. The reference system in which the data are given is stated in 5.1.5 and data sources and usage restrictions are stated in chapter 5.1.4. Gravity gradient grids are described in section 5.2.

The combination of GRACE and GOCE information is done on the gravity gradient level. Since GOCE gravity gradients suffer from a long wavelength error (dominated by 1/f behaviour) this spectral part is being replaced by model gradients. The combination of GOCE and model gradients is being performed under highest priority keeping most valid GOCE information in the gradients. This assumes that also the medium wavelength part will come from GOCE observations (although GRACE can contribute to this spectral regime as well). Model gradients, which are replacing the long wavelength part of the GOCE observations, are being computed from a GRACE/GOCE combined model, namely the GOCO3s (Mayer-Gürr et al., 2012). This model incorporates 8 years of GRACE data and 12 months of GOCE data. Comparing latest GOCE only gravity field models with GOCO03s differences show up between the spherical harmonic coefficients at approximately d/o 140 (which might be due to a higher weight of GRACE information). Since also the difference between the GOCE only solutions (GOCE time-wise and GOCE direct solution R3) is at this spectral regime quite different we stick to the GOCO03s model. Nevertheless this information will only show up in the off diagonal elements of the gravity gradient tensor (see below). The long wavelength gradients, coming from

GOCO03s, have high accuracy. In comparison with combined models such as e.g. EIGEN-6C, GOCO03s shows good error consistency.

For the combined gradients the model gradients and the GOCE observations must be filtered along track. We stick to the suggestion of (Fuchs and Bouman 2011) who claim that the signal to noise of the gradients will be maximized by approximately 5 mHz cut-on frequency which also coincides with the pre-mission specification of the gradiometer. This value could change for the reprocessed data where first tests have shown that especially at the lower MBW the signal quality improves significantly (see also section 5.1.3 below).

After performing a filtering of the gravity gradient observations a complete gravity gradient tensor can be set up for the observations, where the less accurate components (Vxy and Vyz) are set to zero and are replaced by pure model information

$$\bar{V}_{ij}^{G} = \begin{pmatrix} \bar{V}_{XX} & 0 & \bar{V}_{XZ} \\ 0 & \bar{V}_{YY} & 0 \\ \bar{V}_{XZ} & 0 & \bar{V}_{ZZ} \end{pmatrix}$$

The bar above the gradient components indicates that high-pass filtered gravity gradients have been used.

Similar as for the observations a complete gravity gradient tensor can be set up for the computed model gradients. Here the filtered model gradients replace the long wavelength part of the observations indicated by the tilde:

$$\tilde{U}_{ij}^{G} = \begin{pmatrix} \tilde{U}_{XX} & U_{XY} & \tilde{U}_{XZ} \\ U_{XY} & \tilde{U}_{YY} & U_{YZ} \\ \tilde{U}_{XZ} & U_{YZ} & \tilde{U}_{ZZ} \end{pmatrix}$$

The off diagonal elements Vxy and Vyz are completely substituted by model information because here the GOCE gravity gradients have less accuracy (approximately 200x less accurate as compared with the diagonal elements).

A combination of both gravity gradient tensors V and U results in a complete gravity gradient tensor including the long wavelength part of GRACE and the observations from GOCE:

$$V_{ij}^{G} = \bar{V}_{ij}^{G} + \tilde{U}_{ij}^{G}$$

This combined gravity gradient tensor can be rotated to any reference frame using point wise tensor rotation:

$$V_{ab} = RV_{ij}R^{T}.$$

Since the rotational matrix connects the two reference frames via a pre- and post-multiplication, the resulting gravity gradients are a linear combination of the single tensor elements. Therefore model information and observations will be combined. In general this problem can only be circumvented applying the model functionals in the gradiometer reference frame. Note: using rotated gradients model signal and observations will be transferred between the single tensor elements.

### 5.1.1 Data format description

The provided data formats are given by two basic subsets of files. First GRACE/GOCE measured gravity gradients in the gradiometer reference frame (GRF) and second gradients rotated to a terrestrial reference frame (TRF), in particular the spherical local north-oriented frame (LNOF). These data subsets cover the time spans as shown in chapter 5.1.2. The datasets used for this study are provided in roughly monthly intervals. The reference frames are used as stated in chapter 5.1.5. The

files are provided as ASCII standard (File designator .dat) and are provided using the following filename convention:

| ***Filename*** | |
|---|---|
| GGC_GRF_DataFile_#REFGGM#_#STARTDATE_STOPDATE#_#Version-Nr#..dat | FILE Type 1 |
| GGC_TRF_DataFile_#REFGGM#_#STARTDATE_STOPDATE#_#Version-Nr#..dat | FILE Type 2 |

#REFGGM# Indicates the global gravity field solution for data compilation (*by default: GOCO03s*)
#STARTDATE Start date of the measurement period (Table 5-2)
STOPDATE# Stop date of the measurement period (Table 5-2)

#Version-Nr# Version Number of the products (latest version is 0002)

File Type 1 contains the GRF data, file Type 2 contains the TRF data. The file content of the GGC-GRF product is shown in the following.

---

File_Version: 2.0

File_Class: CONS final product
File_Format: ASCII
Mission_Name: GOCE

File_Description: GOCE combined gravity gradients along orbital tracks given in GRF
File_Name: GGC_GRF

Data_Period:
Start-Date (yyyymmdd): 20121101
GPS-Time-Start: 1035763216.9221

Stop-Date (yyyymmdd): 20121107
GPS-Time-Stop: 1036368015.8949

Input_Data:
- EGG: EGG_NOM_2
- Gravity model: GOCO03s (T.M.-Guerr et al., 2011)
- Orbits: SST_PRD (reduced dynamic Orbits)
- Attitude: EGG_IAQ_2C

Data_Descriptor:
(1) GPS-Time in seconds
(2-3) Latitude, Longitude in deg (spherical coord.)
(4) Geocentric radius in meter
(5-10) Combined gradients XX, YY, ZZ, XY, XZ, YZ
(11-16) Gradients along track std. XX, YY, ZZ, XY, XZ, YZ
(17-22) Flags XX, YY, ZZ, XY, XZ, YZ
(23-31) Rotation Matrix GRF2LNOF (R11, R12, R13, R21, R22, R23, R31, R32, R33)

Data_Processing:
GOCE measured gravity gradients are bandpass filtered from 7.5 - 100 mHz for the spectral combination of the GOCE measurements and model derived gradients. Close to the magnetic poles, samples of the Vyy component

```
        are filtered from 15 to 120 mHz to reduce anomalous gradient signal.
        Outliers in the GOCE data have been eliminated using a 3.5 times
        threshold of the along track standard deviation w. r. t the
        background model. Flagged data are being replaced by model derived
        fill ins for the accurate measured gradient data (Vxx, Vyy, Vzz, Vxz).

Flag info: (1) - Valid data
      (2) - Vyy reduced bandwidth data
      (5) - Outlier, fill in provided
      (6) - Outlier, no fill in provided

Some of the processing details are presented in:

Fuchs M., and J. Bouman (2011), Rotation of Gravity
gradients to local frames, Geoph. Journal International, 187, 743-753,
DOI: 10.1111/j.1365-246X.2011.05162.x

end of header
################################################################################
```

**Table 5-0: Header format of the GGC-GRF product**

The first line of the data file is the header line followed by the data. An overview of the data format is given in the following table:

**Table 5-1: Overview of the parameter identifier of the provided file formats**

| Parameter Nr | Parameter identifier | Variable designator | Units | Example data |
|---|---|---|---|---|
| 001 | GPS Time | Float | [s] | 941068815.4... |
| 002 | Latitude | Float | [deg] | 16.99804157... |
| 003 | Longitude | Float | [deg] | 95.26636341... |
| 004 | Radial distance | Float | [m] | 6631233.5710 |
| 005 | Gravity gradient - Vxx | Float | [1/s²] | -1.37173882E-06 |
| 006 | Gravity gradient - Vyy | Float | [1/s²] | -1.36806334E-06 |
| 007 | Gravity gradient - Vzz | Float | [1/s²] | 2.73981266E-06 |
| 008 | Gravity gradient - Vxy | Float | [1/s²] | 1.14089582E-10 |
| 009 | Gravity gradient - Vxz | Float | [1/s²] | 4.61300178E-09 |
| 010 | Gravity gradient - Vyz | Float | [1/s²] | 3.21649476E-10 |
| 011 | Error estimate Vxx | Float | [1/s²] | 1.11671229E-11 |
| 012 | Error estimate Vyy | Float | [1/s²] | 4.04266353E-11 |
| 013 | Error estimate Vzz | Float | [1/s²] | 5.79177168E-11 |
| 014 | Error estimate Vxy | Float | [1/s²] | 8.56139408E-12 |
| 015 | Error estimate Vxz | Float | [1/s²] | 1.03489395E-11 |
| 016 | Error estimate Vyz | Float | [1/s²] | 4.02614024E-12 |
| 017 | Flags Vxx | Integer (0 .. 8) | [1] | 2 |
| 018 | Flags Vyy | Integer (0 .. 8) | [1] | 2 |
| 019 | Flags Vzz | Integer (0 .. 8) | [1] | 2 |
| 020 | Flags Vxy | Integer (0 .. 8) | [1] | 2 |
| 021 | Flags Vxz | Integer (0 .. 8) | [1] | 2 |

| | | | | |
|---|---|---|---|---|
| 022 | Flags Vyz | Integer (0 .. 8) | [1] | 4 |
| 023 | Rotation matrix element R11 | Float | (only for GRF) | (only for GRF) |
| 024 | Rotation matrix element R12 | Float | (only for GRF) | (only for GRF) |
| 025 | Rotation matrix element R13 | Float | (only for GRF) | (only for GRF) |
| 026 | Rotation matrix element R21 | Float | (only for GRF) | (only for GRF) |
| 027 | Rotation matrix element R22 | Float | (only for GRF) | (only for GRF) |
| 028 | Rotation matrix element R23 | Float | (only for GRF) | (only for GRF) |
| 029 | Rotation matrix element R31 | Float | (only for GRF) | (only for GRF) |
| 030 | Rotation matrix element R32 | Float | (only for GRF) | (only for GRF) |
| 031 | Rotation matrix element R33 | Float | (only for GRF) | (only for GRF) |

A total of 31 parameters are given in each file. Note: The trace value for the TRF and GRF gradients can differ since the rotation involves mixing of the off diagonal elements with the measurements of the diagonal elements. The flags (parameters 017 to 022) represent the data quality. Flags between 0 ... 2 indicate valid data. Flags above 2 indicate bad or corrupt data. The parameters 023 to 031 give in combination the rotational matrix R which has to be used for the rotation from the gradiometer reference frame to the terrestrial reference frame. The rotation matrix must be applied to the gravitational tensor as stated above.

### 5.1.2 Spatial and temporal coverage

The GOCE data acquisition covers a time interval starting from the 1st of November 2009 until October 2013. Three major interrupts from data acquisition can be indicated. A first anomaly occurred because of the switch from the erroneous CPU A to CPU B side. A second anomaly led to a two months loss of data due to interference in the satellite acquisition system. Anomaly three was related to the update of the ephemerides table at the start of a new year. The data periods are regularly interrupted by calibration events, which in principle are shaking manoeuvres of the satellite structure. Periods of calibration events are excluded from the nominal data.

On the next page, the distribution of the along-track gravity gradient files in time is shown as well as their relation to the orbital height.

**Table 5-2: GOCE data time line**

| | | Data Period |
|---|---|---|
| 2009 | November | 20091101 – 20091130 |
| | December | 20091201 – 20091231 |
| 2010 | January | 20100101 – 20100111 |
| | | 20100113 – 20100131 |
| | February | 20100201 – 20100212 |
| | | 1st Anomaly |
| | March | 20100307 – 20100319 |
| | | 20100325 – 20100331 |
| | April | 20100401 – 20100430 |
| | May | 20100501 – 20100505 |
| | | 20100509 – 20100531 |
| | June | 20100601 – 20100629 |
| | July | 20100704 – 20100707 |
| | August | 2nd Anomaly |
| | September | 20100911 – 20100912 |
| | | 20100919 – 20100929 |
| | October | 20101002 – 20101004 |
| | | 20101007 – 20101031 |
| | November | 20101101 – 20101130 |
| | December | 20101201 – 20101206 |
| | | 20101212 – 20101231 |
| 2011 | January | 3rd Anomaly |
| | | 20110120 – 20110126 |
| | | 20110129 – 20110131 |
| | February | 20110201 – 20110207 |
| | | 20110211 – 20110228 |
| | March | 20110301 – 20110331 |
| | April | 20110401 – 20110403 |
| | | 20110406 – 20110430 |
| | May | 20110501 – 20110531 |
| | June | 20110601 – 20110606 |
| | | 20110609 – 20110630 |
| | July | 20110701 – 20110731 |
| | August | 20110801 – 20110820 |
| | | 20110825 – 20110831 |

| | | |
|---|---|---|
| 2012 | January | 20120101 – 20120117 |
| | | 20120118 – 20120131 |
| | February | 20120201 – 20120229 |
| | March | 20120301 – 20120305 |
| | | 20120309 – 20120315 |
| | | 20120316 – 20120331 |
| | April | 20120401 – 20120430 |
| | May | 20120501 – 20120522 |
| | | 20120523 – 20120531 |
| | June | 20120601 – 20120606 |
| | | 20120614 – 20120616 |
| | | 20120620 – 20120929 |
| | July | 20120701 – 20120731 |
| | August | 20120801 – 20120831 |
| | | 20120901 – 20120910 |
| | September | 20120912 – 20120930 |
| | October | 20121001 – 20121031 |
| | November | 20121101 – 20121107 |
| | | 20121109 – 20121130 |
| | December | 20121201 – 20121231 |
| 2013 | January | 20130101 – 20130131 |
| | February | 20130201 – 20130204 |
| | | 20130213 – 20130228 |
| | March | 20130301 – 20130331 |
| | April | 20130401 – 20130430 |
| | May | 20130501 – 20130504 |
| | | 20130508 – 20130519 |
| | | 20130530 – 20130531 |
| | June | 20130601 – 20130630 |
| | July | 20130701 – 20130731 |
| | August | 20130804 – 20130831 |
| | September | 20130901 – 20130930 |
| | October | 20131002 – 20131031 |
| | November | 20131101 – 20131105 |

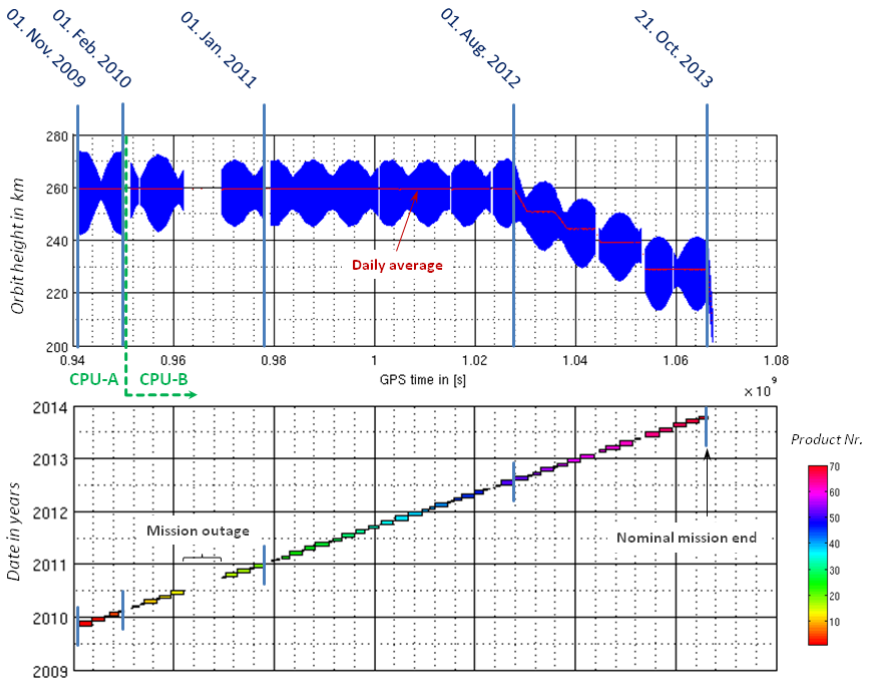


**Top panel shows GOCE orbit height with time. Lower panel shows the distribution of the single gravity gradient files in time.**

The spatial coverage of the GOCE data is determined by the GOCE orbit. GOCE flew approximately at a mean altitude of 260 km above a reference sphere in the nominal phase and had an inclination of 96.5°. Therefore the GOCE ground tracks cover maximum latitude of ~83°. This can be seen from the geographical plot Figure 5-1.

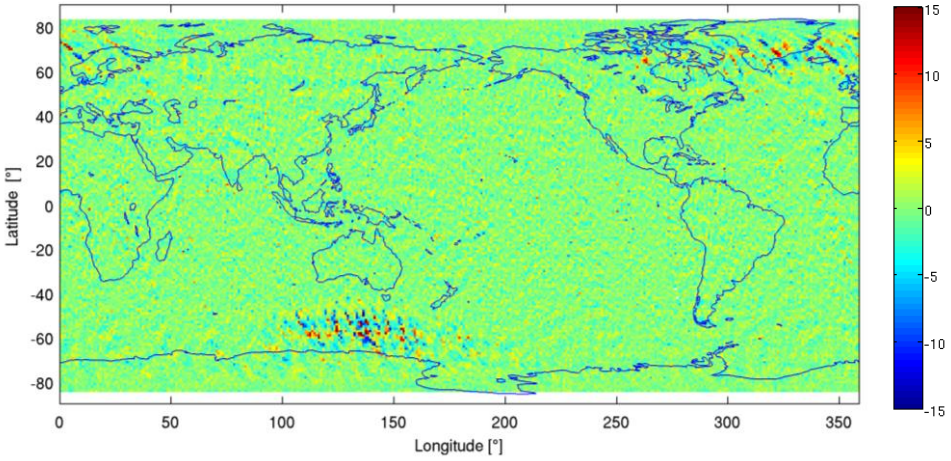


**Figure 5-1: Comparison of GOCE gravity gradients with ITG-GRACE2010S shown for Vyy. Clearly anomalous tracks at the magnetic poles can be seen.**

### 5.1.3 Data strengths and weaknesses

The data periods do not differ significantly in the error properties of the global analysed gravity gradients inside the measurement bandwidth, except for the period before and after the February anomaly which occurred in 2010. Figure 5-2 shows an analysis of residuals to the reference model GOCO03s of the diagonal gravity gradient components over time. A switch from the CPU A to the CPU B-side had impacts on the error characteristics of Vzz, Vyy and Vxx, where the most change in gradient quality can be indicated for Vzz (dashed arrow). The residuals to a reference model decrease there by approximately a factor of 1.5 for Vzz.

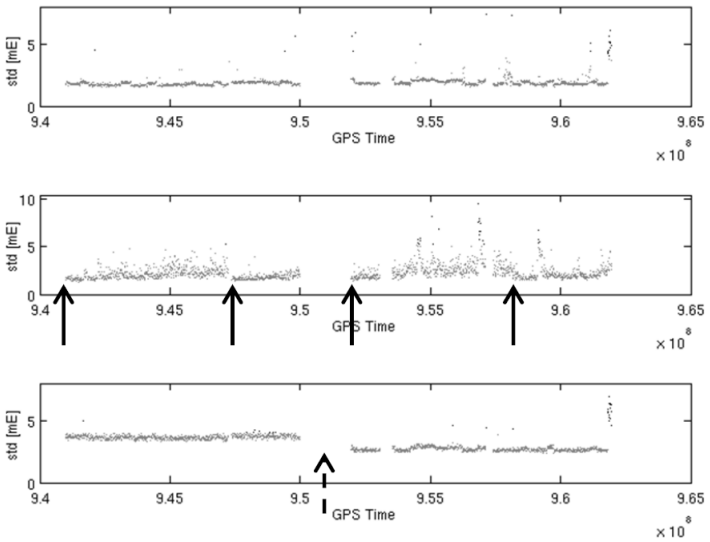


**Figure 5-2: Residuals for Vxx (top) Vyy (middle) and Vzz (bottom) over time. The residuals have been computed in intervals of 10,000 samples. The arrows in the middle plot indicate calibration events, while the dashed arrow indicates the CPU switch.**

There was a drift in the scaling parameters of the instrument which results in a leakage of common mode accelerations onto the measurements. Especially in the Vyy component it can be seen that this leakage has influence on the error properties of the measurements. Because the cross-track

component has no drag compensation, in contrast to Vxx, cross track thermospheric winds can influence the gradient quality. For satellite positions close to the magnetic poles clearly the higher noise in the gradients can be indicated (see Figure 5-1).

This problem was improved for reprocessed gravity gradients. First tests with the new processor version have shown that especially in the Vyy component at the poles and in the spectral analysis (at the lower measurement bandwidth) improvements can be indicated (see Figure 5-3). The new developed processor makes use of an improved angular rate reconstruction, considering all three on-board star trackers and a Wiener filter with less warm up time compared with the previous used Kalman filter. Nevertheless, the Vyy problem is persistent to some extent and in the combination of GRACE/GOCE we used an adaptive procedure. Close to the magnetic poles the GOCE Vyy data are combined with GOCO03s using a filter of 15 mHz. Away from the magnetic poles we use 5 mHz as is used for the other accurate gradients. A smooth transition from 15 to 5 mHz is used depending on the distance to the magnetic poles.

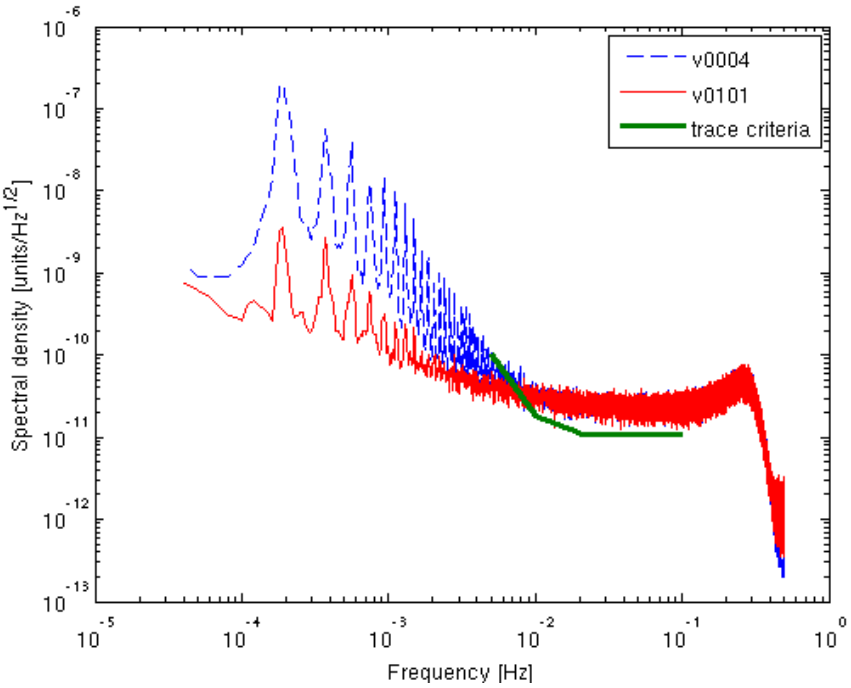


**Figure 5-3: Improvements in the gravity gradient trace for the new processor version v0101 with respect top the old version v0004 (version numbers refer to Level 2 data).**

### 5.1.4 Data source and usage restrictions

The raw data products provided by ESA have been used as input dataset and are being enriched by processing routines resulting in modified gravity gradients which have been processed in-house at DGFI. These products do not underlie special restrictions.

### 5.1.5 Reference systems in use

The GOCE measurements are referred to the gradiometer reference frame (GRF) which is fixed with the satellite's structure. Since the satellite rotates around the Earth, deviations from the GRF to the orbital reference frame (LORF spanned by the velocity and the radial vector) are usual within the mission pre-specification. The on-board magnetic torquers and the ion engine on board of GOCE are used to establish a quite smooth guidance of the satellite around its orbit. Figure 5-4 shows the deviation of the satellite's attitude with respect to two reference frames LORF-v and LNOF (Fuchs and Bouman 2011).

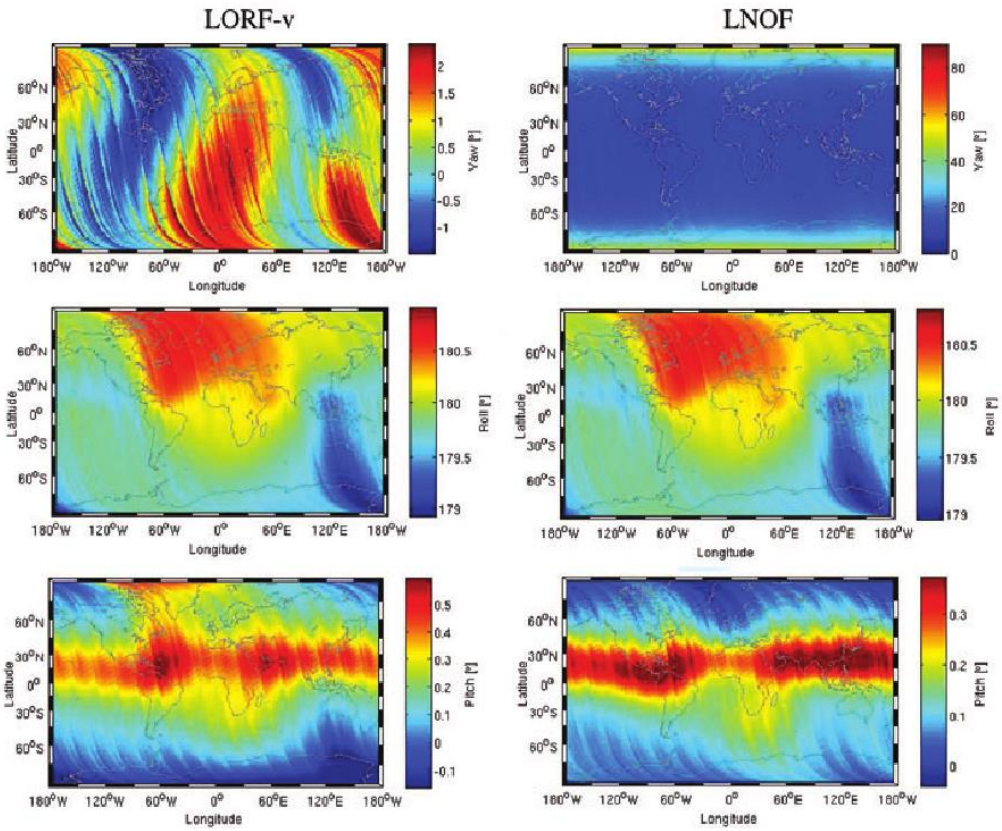


**Figure 5-4: Deviations of the satellite's attitude with respect to the gradiometer reference frame for ascending tracks. (left) LORF-v (right) LNOF**

This deviation has to be considered when rotating the gravity gradients onto a chosen reference frame. Figure 5-5 shows the gradiometer reference frame given in the orbital frame. In this reference frame the observations are being generated. Using the deviations from the orbital reference frame (LORF-v) and the rotation of the LORF-v onto the terrestrial (Earth fixed reference frame) a rotational matrix can be set up which directly rotates between the GRF and the LNOF. This matrix (see also last paragraph 5.1.1) provided in the GRF data file is being used for the rotation between the two reference systems.

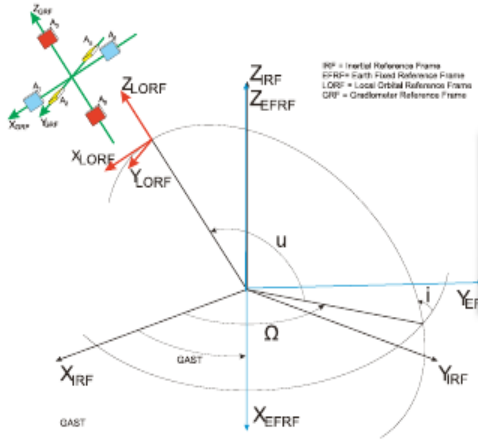


**Figure 5-5: Principle sketch of the gradiometer orientation with respect to the EFRF frame and LORF**

### 5.1.6 Error information

With the provided gravity gradient data, error estimates of the gradients are being delivered. According to these error estimates the gradient accuracy can be evaluated using the latest GOCE gravity field models. In principle this analysis reveals that the gravity gradient accuracy is good. Figure 5-6 shows a Power Spectral Density (PSD) of the GOCE gravity gradients for a time period covering one complete repeat cycle.

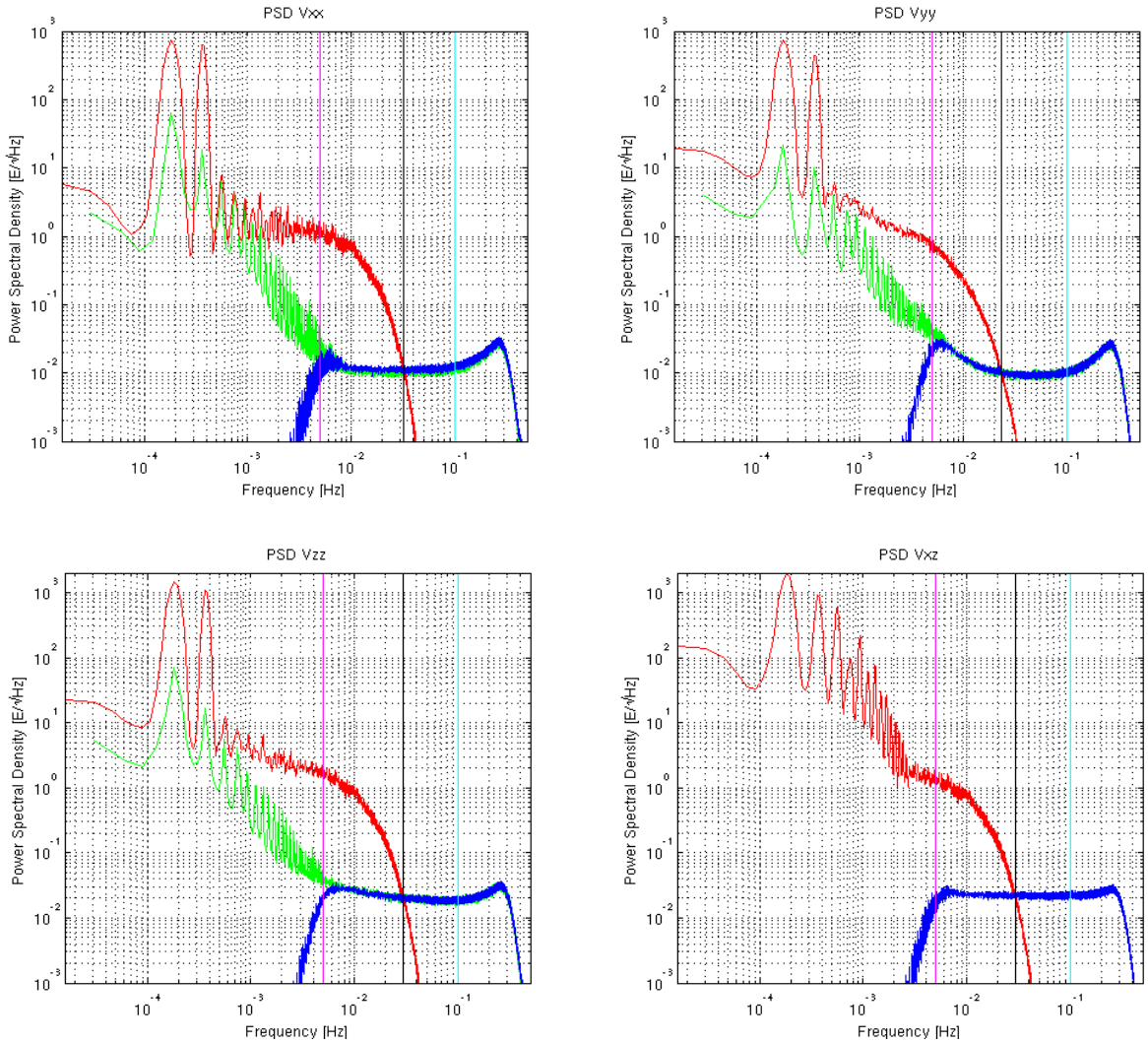


**Figure 5-6: Error PSD for different gravity gradients; (green) estimated error PSD of the quick-look processing, (red) model signal, (blue) high pass filtered observation residuals**

In green the estimated quick-look error PSD is being shown for the diagonal tensor elements (Note: Vxz is not being considered in the QL estimation process). From this error PSD clearly the 1/f error behaviour can be seen. Comparing the gradient residuals with the error PSD it can be stated that these estimates are quite consistent with the residuals coming from a reference model. Also from the error PSD plots and the residual plots it is obvious that the noise in the Vzz component is twice as large as compared to Vxx and Vyy. Nevertheless Vzz has also double signal energy. The error behaviour is not fully understood.

## 5.2 Gravity gradient grids

### 5.2.1 LNOF – Local North Oriented Frame

Grids of gravity gradients are provided in the LNOF above the ellipsoid. The gradient grids are given on a homothetic ellipsoid that has the same eccentricity as the WGS84 ellipsoid and a semi-major axis $a_H = a_{WGS84} + H$, where $a_{WGS84}$ = 6378.137 km and $H$ is 225 km or 255 km. In practice this means that the height $h$ above the WGS84 ellipsoid slightly varies from equator to the poles. For the lower grids, for example, the height is $h$ = 225 km at the equator and $h \approx 224.25$ km at the poles. The LNOF is defined using geocentric longitude $\lambda$ and latitude $\phi$ and we have

$$Z_{LNOF} = \begin{pmatrix} \cos\phi\cos\lambda \\ \cos\phi\sin\lambda \\ \sin\phi \end{pmatrix}; Y_{LNOF} = \begin{pmatrix} \sin\lambda \\ -\cos\lambda \\ 0 \end{pmatrix}; X_{LNOF} = \begin{pmatrix} -\sin\phi\cos\lambda \\ -\sin\phi\sin\lambda \\ \cos\phi \end{pmatrix},$$

The origin is located at the grid point, $Z_{LNOF}$ is defined as the vector from the geocenter to the origin (grid point), pointing radially outward, $Y_{LNOF}$ is parallel to the normal vector to the plane of the geocentric meridian of the satellite center of mass, pointing westward, $Z_{LNOF}$ points North and is parallel to the normal vector to the plane defined by $Y_{LNOF}$ and $Z_{LNOF}$ and forms a right-handed system. (X, Y, Z) is therefore (N, W, U) = North, West, Up.

Geocentric coordinates $(r, \phi, \lambda)$ are used for a sphere whereas geographic (or geodetic) coordinates $(h, \varphi, \lambda)$ are used for the ellipsoid. The longitude $\lambda$ is the same in both coordinate systems, whereas geodetic and geocentric latitude differ. This is shown in the Figure below.

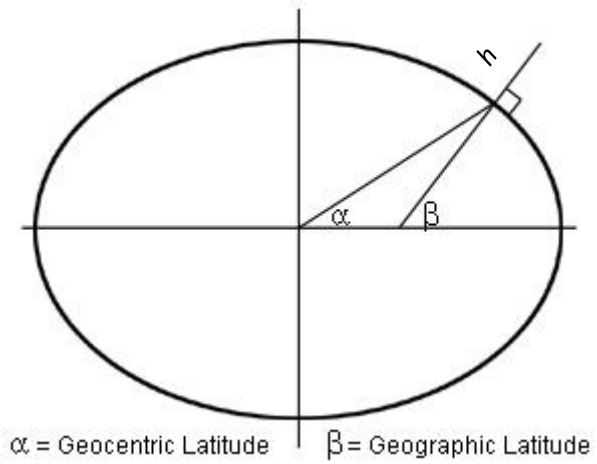


**Figure: Geocentric latitude $\phi$ ($\alpha$ in the figure), geodetic latitude $\varphi$ ($\beta$ in the figure) and height $h$ above the ellipsoid.**

One obtains the Cartesian coordinates (x, y, z) of the grids from the given $(\lambda, \varphi)$as follows:

$$x = N\cos\varphi\cos\lambda$$
$$y = N\cos\varphi\sin\lambda$$
$$z = N(1-e^2)\sin\varphi$$

with $N = (a_{WGS84} + H)(1 - e^2\sin^2\varphi)^{-\frac{1}{2}}$, where, as stated above, $a_{WGS84}$ is the WGS84 semi-major axis, $e$ is the WGS84 eccentricity and $H$ is 225 km or 255 km.

The Cartesian coordinates (x, y, z) are related to geocentric coordinates $(r, \lambda, \phi)$ as

$$x = r\cos\phi\cos\lambda$$
$$y = r\cos\phi\sin\lambda$$
$$z = r\sin\phi$$

with the inverse relations

$$r = \sqrt{x^2 + y^2 + z^2}$$
$$\lambda = \operatorname{atan}\frac{y}{x}$$
$$\phi = \operatorname{asin}\frac{z}{r}$$

### 5.2.2 Grid format

Gravity gradient grids at 225 km and 255 km above the ellipsoid have been computed using as input the GRACE-GOCE gravity gradients along the orbit. First regional grids were computed using the tesseroid approach as described in the Algorithm Theoretical Basis Document. The patchwork of regional grids was then used to compute global grids. The format of the grids is given in the table below. In each row we have longitude and latitude in degrees and then $V_{XX}$, $V_{XY}$, $V_{YZ}$, $V_{ZZ}$, $V_{YZ}$, $V_{YY}$ in E (Eötvös, 1 E = $10^{-9}$ $s^{-2}$). The height above the ellipsoid is indicated in the file name.

Data from the nominal mission have been used to compute the grids at 255 km, data from the extended missing phase have been used to compute the grids at 225 km. Note that geographic coordinates are used for the grid definition, which thus slightly differs from the spherical definition because geocentric and geographic latitude are slightly different.

| **Header information (given below)** | | | | | | | | | | | | | |
|---|---|---|---|---|---|---|---|---|---|---|---|---|---|
| *Geographic coordinates (degree)* | | *Gravity gradients in the LNOF (Eötvös) (X = North, Y = West, Z = Up)* | | | | | | *Estimated errors (Eötvös)* | | | | | |
| Longitude | Latitude | $V_{XX}$ | $V_{XY}$ | $V_{XZ}$ | $V_{ZZ}$ | $V_{YZ}$ | $V_{YY}$ | $V_{XX}$ | $V_{XY}$ | $V_{XZ}$ | $V_{ZZ}$ | $V_{YZ}$ | $V_{YY}$ |

```
File_Version: Release 1.0

File_Class: CONS final product
File_Format: ASCII
Mission_Name: GOCE

File_Description: GOCE/GRACE combined gravity gradient grids at fixed height above ellipsoid given
in LNOF(defined in geocentric coordinates), reference values from WGS84 were subtracted. X =
North, Y = West, Z = Up.
File_Name: GGC_GRF

 Data_Period:
   Start-Date (yyyymmdd):  20121101
   GPS-Time-Start:  1035763216.9221

   Stop-Date (yyyymmdd):  20121107
   GPS-Time-Stop:  1036368015.8949

 Input_Data:
         - EGG: GOCE/GRACE gradients similar to GGC_GRF
         - Gravity model: GOCO03s (T.M.-Guerr et al., 2011)
         - Orbits: SST_PRD (reduced dynamic Orbits)
         - Attitude: EGG_IAQ_2C

 Data_Descriptor:
        (1) Longitude in degree (geographic coordinates)
        (2) Latitude in degree (geographic coordinates)
            Approximate height above the ellipsoid in km is indicated in the file name
      (3-8) Gravity gradients XX, XY, XZ, YY, YZ, ZZ in the LNOF (in Eötvös)
     (9-14) Estimated gravity gradient errors XX, XY, XZ, YY, YZ, ZZ (in Eötvös)

 Data_Processing:
         GOCE/GRACE gravity gradients in the GRF are reduced with GOCO03s model values
         These residuals are used to estimate residual densities in tesseroids of 0.5 degree in blocks
         of 15 times 15 degree. The residual densities are used to computed gravity gradient
         corrections to GOCO03s at 225 km or 255 km above the sphere in equal area blocks. A
         global patchwork is obtained by interpolation to 0.2 degree equiangular grids. With
         spherical harmonic analysis spherical harmonic coefficients are derived, which are used to
         compute gravity gradients in equiangular grids on a homothetic ellipsoid that has the same
         eccentricity as the WGS84 ellipsoid and a semi-major axis a_H = a_WGS84 + H, where
         a_WGS84 = 6378.137 km and H is 225 km or 255 km. In practice this means that the height h
         above the WGS84 ellipsoid slightly varies from equator to the poles. For the lower grids, for
         example, the height is h = 225 km at the equator and h ≈ 224.25 km at the poles.
         Using the Poisson Integral Equation for downward and upward continuation, corrections to
         the gravity gradients are estimated in an iterative procedure. Applying these will reduce the
         errors.

end of header
################################################################################
```

**Table: Header format of the gravity gradient grids**

### 5.2.3 Error estimation

Using the Poisson integral equation (PIE) it is possible to iteratively predict gravity gradient grids at the Earth's surface using the grids at satellite altitude as input (Sebera et al. 2014). In addition, the iterative procedure allows estimating the errors of the grids at satellite altitude by comparing the reproduced grids at satellite altitude and the given grids. These estimated errors are given in columns 9 – 14 of the grid data files. Note that by subtracting these estimated errors from the gradients 3 – 8 the error is reduced, but it might also reduce the signal.

The differences between the grids and recent state-of-the-art global gravity field models are shown in Figure 5 for the vertical gravity gradient. GOCO03s was used as reference model and the differences with the grids are caused on the one hand by data errors and on the other hand by additional signal content that may be contained in the grids. We note that at long wavelengths the grids cannot improve upon the reference model as we perform regional gravity field analysis. The differences increase towards the south for both the 225 km and 225 km grids, which is caused by the greater orbit height in the southern hemisphere. As said above, in an iterative downward continuation procedure the errors in the grids were estimated. In effect, the grids are low-pass filtered, which reduces noise but also might reduce signal. If we reduce the noise from the grids we see that the differences with GOCO03s become more homogeneous (Figure 5B and C). EGM2008 is a state-of-the-art high resolution global gravity field model that does not contain GOCE data. Instead, it combines GRACE, terrestrial gravity data and satellite altimeter data. We see that there are large differences over the continents in regions where terrestrial gravity data are sparse. In addition, the signature of the Antarctic Circumpolar Current is visible, which is caused by the imperfect separation of geoid and dynamic ocean topography signal from satellite altimetry in EGM2008. This emphasizes the significance of GOCE for improved gravity field determination.

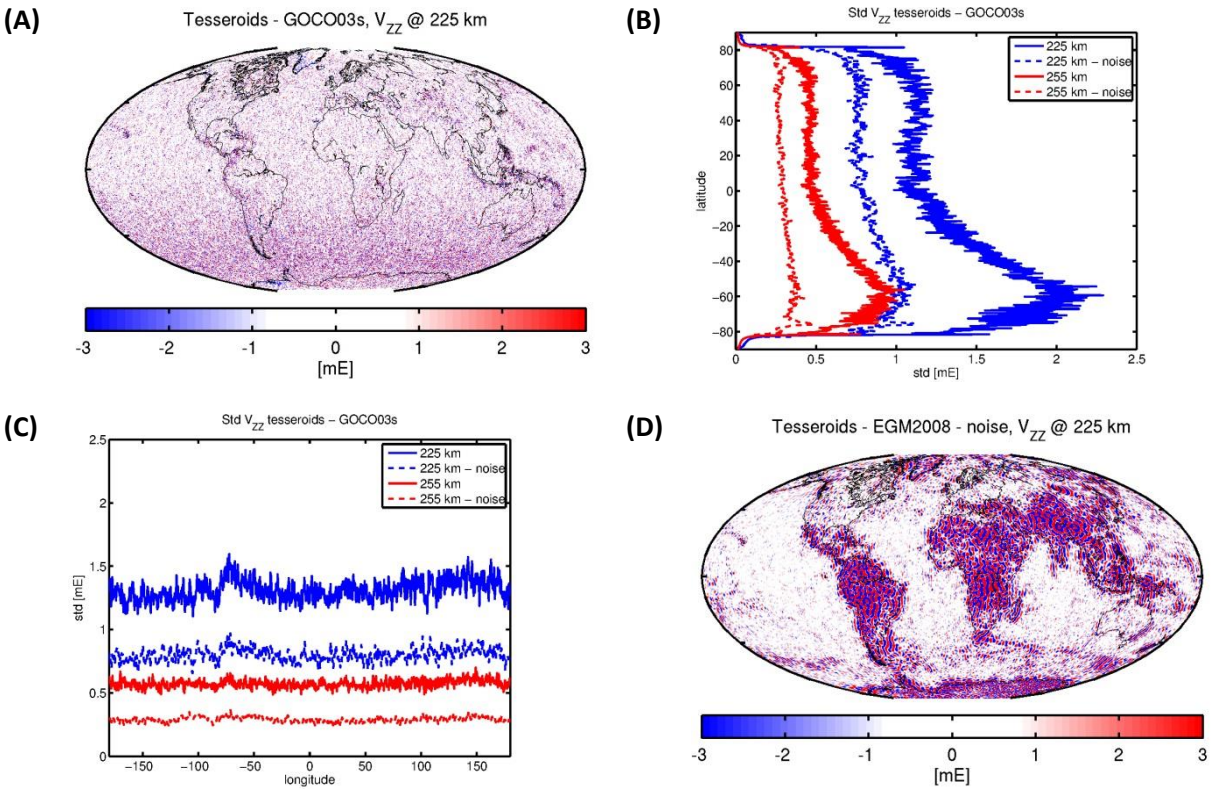


**Figure 5: $V_{ZZ}$ differences to GOCO03s and EGM2008: (A) Tesseroids – GOCO03s @ 225 km; (B) Standard deviation as function of latitude @ 225 and 255 km, with and without noise reduction; (C) Standard deviation as function of longitude @ 225 and 255 km, with and without noise reduction; (D) Tesseroids – EGM2008, noise reduced.**

### 5.2.4 Topographic reduction

Gravity gradients are also provided that are based on the topographic potential (Grombein et al. 2013, 2014). These "topographic" gravity gradients are provided in the same grid points as the 225 km and 255 km GOCE/GRACE gravity gradient grids, and can be used for a topographic reduction of the observed gravity gradients. Note that it is not really a "reduction" because only the topography is used, not the isostatic compensation. Thus the signal will increase after topographic reduction, similar to the computation of Bouguer gravity anomalies.

| **Header information (given below)** | | | | | | | |
|---|---|---|---|---|---|---|---|
| *Geographic coordinates (degree)* | | *Gravity gradients in the LNOF (Eötvös) (X = North, Y = West, Z = Up)* | | | | | |
| Longitude | Latitude | $V_{XX}$ | $V_{XY}$ | $V_{XZ}$ | $V_{ZZ}$ | $V_{YZ}$ | $V_{YY}$ |

File_Version: Release 1.0

File_Class: CONS final product
File_Format: ASCII
Mission_Name: GOCE

File_Description: Gravity gradient grids from topography at fixed height of 225 km above ellipsoid given in LNOF
File_Name: GO_CONS_TGG_225_KI12_20120801T000000_20131111T235959_0001.TGZ (Global GOCE gravity gradient grids above the ellipsoid for geophysical and geodetic applications)

Data_Period:
Start-Date (yyyymmdd): 20121101
GPS-Time-Start: 1035763216.9221

Stop-Date (yyyymmdd): 20121107
GPS-Time-Stop: 1036368015.8949

Input_Data:

- RWI_TOPO_2012_plusGRS80 (Topographic potential + GRS80)
- References:
  Grombein, T.; Luo, X.; Seitz, K.; Heck, B. (2014): A wavelet-based assessment of topographic-isostatic reductions for GOCE gravity gradients. Surveys in Geophysics 35(4):959-982, DOI: 10.1007/s10712-014-9283-1
  Grombein, T.; Seitz, K.; Heck, B. (2013): Optimized formulas for the gravitational field of a tesseroid. Journal of Geodesy 87(7):645-660, DOI: 10.1007/s00190-013-0636-1

Data_Descriptor:
(1) Longitude in degree (geographic coordinates)
(2) Latitude in degree (geographic coordinates)
Approximate height above the ellipsoid in km is indicated in the file name
(3-8) Gravity gradients XX, XY, XZ, YY, YZ, ZZ in the LNOF (in Eötvös)

Data_Processing:
Topographic spherical harmonic coefficients are used to compute gravity gradients in equiangular grids of 0.2 degree on a homothetic ellipsoid that has the same eccentricity as the WGS84 ellipsoid and a semi-major axis a_H = a_WGS84 + H, where a_WGS84 = 6378.137 km and H is 225 km or 255 km. In practice this means that the height h above the WGS84

```
        ellipsoid slightly varies from equator to the poles. For the lower grids, for example, the
        height is h = 225 km at the equator and h ~224.25 km at the poles. The gradients in this file
        can be used for topographic reduction of the GOCE/GRACE at 225 km.

end of header
#################################################################################
```

# 6 References


Bruinsma S, Marty J, Balmino G, Biancale R, Foerste C, Abrikosov O and Neumayer H (2010) GOCE Gravity Field Recovery by Means of the Direct Numerical Method, presented at the ESA Living Planet Symposium, 27th June - 2nd July 2010, Bergen, Norway

Förste C, S Bruinsma, R Shako, J Marty, F Flechtner, O Abrikosov, C Dahle, J Lemoine, H Neumayer, R Biancale, F Barthelmes, R König and G Balmino (2011) EIGEN-6 - A new combined global gravity field model including GOCE data from the collaboration of GFZ-Potsdam and GRGS-Toulouse, Geophysical Research Abstracts Vol. 13, EGU2011-3242-2, 2011

Fuchs M, Bouman J (2011) Rotation of GOCE gravity gradients to local frames. Geophysical Journal International, 187, 743–753, DOI: 10.1111/j.1365-246X.2011.05162.x

Goiginger H, Hoeck E, Rieser D, Mayer-Guerr T, Maier A, Krauss S, Pail R, Fecher T, Gruber T, Brockmann J, Krasbutter I, Schuh W, Jaeggi A, Prange L, Hausleitner W, Baur O, Kusche J: (2011) The combined satellite-only global gravity field model GOCO02S, presented at the 2011 General Assembly of the European Geosciences Union, Vienna, Austria, April 4-8

Grombein, T.; Luo, X.; Seitz, K.; Heck, B. (2014): A wavelet-based assessment of topographic-isostatic reductions for GOCE gravity gradients. Surveys in Geophysics 35(4):959-982, DOI: 10.1007/s10712-014-9283-1

Grombein, T.; Seitz, K.; Heck, B. (2013): Optimized formulas for the gravitational field of a tesseroid. Journal of Geodesy 87(7):645-660, DOI: 10.1007/s00190-013-0636-1

Pail R, Bruinsma S, Migliaccio F, Förste C, Goiginger H, Schuh WD, Höck E, Reguzzoni M, Brockmann JM, Abrikosov O, Veicherts M, Fecher T, Mayrhofer R, Krasbutter I, Sansò F, Tscherning CC (2011) First GOCE gravity field models derived by three different approaches, J Geod, doi: 10.1007/s00190-011-0467-x

Pavlis N, Holmes S, Kenyon S, Factor J (2008) An Earth Gravitational Model to Degree 2160: EGM2008, Presented at the EGU General Assembly 2008, Vienna, Austria

J Sebera, M Šprlák, P Novák, A Bezděk, M Vaľko (2014) Iterative Spherical Downward Continuation Applied to Magnetic and Gravitational Data from Satellite, Surveys in Geophysics